

Electronic power transfer in pulsed laser excitation of polar semiconductors

W. Pötz* and P. Kocevar

Institut für Theoretische Physik, Universität Graz, A-8010 Graz, Austria

(Received 9 March 1983)

A time-resolved transport analysis of highly nonequilibrium photoexcited carrier-phonon systems is presented. It is shown that amplification of the most strongly coupling optical-phonon modes leads to a drastic reduction of the intraband cooling rates of the electron-hole plasma. As a consequence and in contrast to earlier expectations, free-carrier screening of the long-range Fröhlich couplings turns out to play only a secondary role. The theory is free of adjustable parameters and in qualitative agreement with hitherto unexplained experimental results from time-resolved transmission spectroscopy of gallium arsenide.

I. INTRODUCTION

The initial energy relaxation of laser-excited electrons and holes in gallium arsenide from higher portions of the central band valleys to their respective band extrema has been recently studied by time-resolved transmission^{1,2} and luminescence^{3,4} spectroscopy at low temperatures. The experimentally determined carrier temperatures revealed that the cooling rates during the first 10–100 psec after a 0.5-psec excitation pulse where only 50% of the theoretical expectations as obtained from a calculation of the power loss due to emission of optical phonons through free-carrier screened polar Fröhlich couplings.¹ The existence of a carrier temperature T_c common to both electrons and holes was experimentally justified by giving reasonable fits to the transmission data in terms of Fermi-Dirac distributions of the carriers.

The remaining discrepancies were believed to be caused by a partial heating of the longitudinal-optical (LO) phonon system, and some authors suggested fitting the experimental cooling rates by introducing a phenomenological phonon temperature into the standard expressions for phonon equilibrium.^{5,6}

A more detailed transport analysis of the highly nonequilibrium coupled systems of electrons, holes, LO and transverse-optical (TO) phonons is presented in Secs. II and III. It is free of any adjustable parameter, gives qualitative agreement with experiment, and shows that LO-phonon amplification indeed plays the decisive role for the low cooling rates, although in an unexpected, indirect manner. Since this aspect might be of relevance for the recent discussion of the role of free-carrier screening in pulsed-laser annealing, we have also extended the present theory to a preliminary investigation of quasicontinuous laser excitation (Sec. IV).

II. THEORY

Following earlier work on nonequilibrium carrier-phonon systems in dc transport,⁷ we start from the rate equation for the total carrier energy E per unit volume and from the Boltzmann equation for the mean occupation numbers $N_{\beta, \vec{q}}(t)$ of the electronically excited phonon

modes of wave vector \vec{q} and branch index β .

The rate equation

$$\frac{dE(t)}{dt} = \left[\frac{dE}{dt} \right]_L + \left[\frac{dE}{dt} \right]_{\text{Aug}} + \left[\frac{dE}{dt} \right]_{\text{ph}} + \left[\frac{dE}{dt} \right]_{\text{rec}} \quad (1)$$

contains the power input from the laser during the pulse and from nonradiative Auger recombinations, the direct energy exchange between the carriers and the lattice through emission and absorption of phonons and the electron-hole ($e-h$) recombination losses.

The energy gain from the laser can be deduced from the experimentally determined pair concentration. It consists of direct one-photon absorption (D1PA), two-photon absorption (D2PA), free-carrier absorption (FCA), and direct intervalence-band absorption processes:

$$\left[\frac{dE}{dt} \right]_L = \left[\frac{dE}{dt} \right]_{\text{D1PA}} + \left[\frac{dE}{dt} \right]_{\text{D2PA}} + \left[\frac{dE}{dt} \right]_{\text{FCA}} + \left[\frac{dE}{dt} \right]_{\text{IV}} \quad (2)$$

The power input from the dominant direct interband absorption can be written in terms of the pair-generation rate G , the energy gap E_g , the photon energy $h\nu$, and the laser pulse length t_p as

$$\left[\frac{dE}{dt} \right]_{\text{D1PA}} = G(t)(h\nu - E_g), \quad 0 \leq t \leq t_p \quad (3)$$

In view of the experimental uncertainties in the determination of the pair densities n we neglect the influence of the pulse shape on $G(t)$. For picosecond excitation we assume G to be a constant, given by

$$G_0 = \frac{n(t_p)}{t_p}, \quad 0 \leq t \leq t_p \quad (4)$$

For cw excitation, effects of band filling must be taken into account, leading to

$$G(t) = G_0[1 - f_e(\epsilon_e, t) - f_h(\epsilon_h, t)], \quad (5)$$

where f is a heated Fermi distribution for electrons and holes of energy

$$\epsilon_{e,h} = (h\nu - E_g) \frac{m_{h,e}}{m_e + m_h}, \quad (6)$$

with effective masses m_e and m_h .

The power input from two-photon absorption is taken as

$$\left[\frac{dE}{dt} \right]_{D2PA} = \beta \frac{G^2 h\nu}{2\alpha_0^2} (2h\nu - E_g), \quad 0 \leq t \leq t_p. \quad (7)$$

With $\beta(\text{GaAs}) \approx 3 \times 10^{-15}$ cm sec/erg (Ref. 8) and with the absorption coefficient $\alpha_0 = 10^4$ cm $^{-1}$ (Ref. 9), these processes are negligible for carrier densities below 10^{21} cm $^{-3}$.

The contributions of free-carrier absorption,

$$\left[\frac{dE}{dt} \right]_{FCA} = h\nu G(t) \frac{\alpha_{FCA}}{\alpha_0}, \quad (8)$$

were estimated using the experimental value $\alpha_{FCA} = \alpha_0 n (5 \times 10^{-23} \text{ cm}^3)$ for germanium,¹⁰ assuming no pronounced differences in the absorption dynamics of GaAs and Ge for the photon energies of our analysis. Direct inter-valence-band transitions between heavy- and light-hole bands and the split-off band were neglected because of the small combined densities of state and the low hole Fermi levels.

In every radiationless Auger recombination event, the energy E_g is added to the carrier plasma; the corresponding rate can be written as

$$\left[\frac{dE}{dt} \right]_{Aug} = E_g C' n^3, \quad (9)$$

with $C' = 10^{-31}$ cm 6 sec $^{-1}$ for GaAs.¹¹

Free-carrier absorption and Auger recombination are negligible for ultrashort excitation pulses, but play a noticeable role in the approach to a steady state during quasicontinuous excitation, particularly when band-filling effects reduce the direct interband absorption.

For the carrier concentrations and temperatures of our analysis, the relaxation times for intercarrier scattering can be estimated¹² to be $\tau_{e-e} \leq 10^4 n^{-1} < \tau_{e-h} < \tau_{h-h} \lesssim 3 \times 10^4 n^{-1}$. These estimates support the experimental evidence for the establishment of a carrier temperature, because all other characteristic times like the pulse length or the relaxation times for carrier-phonon scattering [as inferred from Eq. (20) below] are larger.

Our neglect of collective plasma effects might become questionable for our preliminary estimate of quasi-cw excitation in Sec. IV, with pair densities of 5×10^{19} cm $^{-3}$. But the presence of mixed plasmon-phonon modes would not drastically change the overall energy relaxation of the carriers, because the energy within the plasmon part of these modes will remain in the electron-hole system. Nevertheless, collective plasma effects might play a noticeable role, as was recently shown for laser-excited cadmium-selenide.¹³

The direct energy transfers between the carriers (c) and the lattice through emission and absorption of phonons is

given by

$$\left[\frac{dE}{dt} \right]_{ph} = - \sum_j^{\text{modes}} \sum_i^{\text{coupling}} \hbar\omega_j \left[\frac{dN_j(t)}{dt} \right]_{c,i}, \quad (10)$$

with mode index $j = (\beta, \vec{q})$.

In tetrahedral direct-gap III-V compounds both types of zone-center carriers couple to LO phonons through the polar-optical (PO) interaction and to longitudinal- and transverse-acoustical modes through the acoustic-deformation potential (ADP) and piezoelectric (PZ) coupling, whereas only holes couple to TO modes, via the optical-deformation potential (ODP).⁵

The contributions of the acoustical modes to Eq. (10) are negligible during the initial downward relaxation of the carriers towards the band extrema, but their relative importance increases when the carriers have reached a temperature for which most carriers have energies less than $\hbar\omega_{LO,TO}$ above the bottom of their bands.

The phonon distribution functions and their rate of change in Eq. (10) are calculated from the Boltzmann equation, which includes also the nonelectronic phonon dissipation mechanisms:

$$\frac{dN_j(t)}{dt} = \sum_i^{\text{coupling}} \left[\frac{dN_j(t)}{dt} \right]_{c,i} + \left[\frac{dN_j(t)}{dt} \right]_{\text{nonelec}}. \quad (11)$$

Owing to the experimentally established Fermi distributions, the carrier-phonon collision integrals can be solved in closed form to give the emission and absorption rates as functions of the instantaneous carrier temperature $T_c(t)$ and of the chemical potentials $\mu_e(t)$ and $\mu_h(t)$ (in fact the holes will be nondegenerate in most of the following examples):

$$\left[\frac{dN_j(t)}{dt} \right]_{c,i} = \sum_s^{e,h} [(N_j(t) + 1) E_{i,j}^{(s)} - N_j(t) A_{i,j}^{(s)}], \quad (12)$$

with the emission and absorption rates given by¹⁴

$$E_{i,j}^{(s)} = \frac{m_c^2 k T_c}{\pi \hbar^4} \frac{e^{-W_j}}{1 - e^{-W_j}} \frac{B_{i,j}^{(s)}(q)}{q} \ln \frac{\kappa_s e^{(W_j - z_s^2)/4z_s^2} + 1}{\kappa_s e^{(W_j - z_s^2)/4z_s^2} + e^{-W_j}} \quad (13)$$

and

$$A_{i,j}^{(s)} = E_{i,j}^{(s)} e^{W_j}. \quad (14)$$

We have used dimensionless phonon energies $W_j = \hbar\omega_\beta(q)/kT_c$ and momenta $z_s = q/(2m_s kT_c)^{1/2}$, and the abbreviation $\kappa_s = \exp(-\mu_s/kT_c)$. The carrier-phonon couplings $B_{i,j}^{(s)}$ are defined by the transition amplitudes of the interaction Hamiltonian $H_{i,j}$ for emission and absorption processes⁷:

$$B_{i,j}^{(s)} = |(\vec{p} \mp \vec{q}, N_j \pm 1 | H_{i,j}^{(s)} | \vec{p}, N_j)|^2 (N_j + \frac{1}{2} \pm \frac{1}{2})^{-1}. \quad (15)$$

These couplings must include possible screening effects due to free carriers. A sum of Thomas-Fermi or (in case of nondegeneracy) of Debye-Hückel susceptibilities will properly describe the free-carrier screening of the long-range polar interaction for the small- q intravalley transitions considered here.^{5,15} The screening of the short-range

optical-deformation potentials of the holes represents a more subtle problem. The Thomas-Fermi contribution to the leading zero-order term of the general q expansion of the phonon-induced transition probability vanishes by symmetry, so that any screening effects of free carriers will be due to the higher-order terms, for which no definitive screening prescription can be given. In our numerical analysis these screening corrections were neglected; however we will show one calculation for a fully Thomas-Fermi screened optical-deformation potential in order to demonstrate that even in this (unrealistic) case the reduction of the short-range ODP couplings is much less effective than for the long-range PO interaction, which is dominated by $q \approx 0$ transitions.

For the nonelectronic phonon losses we have used the well-established relaxation-time ansatz

$$\left(\frac{dN_j(t)}{dt} \right)_{\text{nonelec}} = - \frac{N_j(t) - N_j^{(0)}}{\tau_j(T_L)} \quad (16)$$

towards the equilibrium Planck distribution $N_j^{(0)}$, at lattice temperature T_L , with experimentally determined phonon lifetimes $\tau_j(T_L)$.¹⁶ For the optical modes a value of $\tau_{\text{op}}(0) = 26$ psec in the semiempirical interpolation formula of Klemens,¹⁷

$$\tau_{\text{op}}(T_L) = \tau_{\text{op}}(0) \left[1 + 2 \left[\exp \frac{\hbar\omega_j}{2kT_L} - 1 \right]^{-1} \right]^{-1}, \quad (17)$$

leads to τ values somewhat below the longest experimental low-temperature LO phonon lifetimes (of ≈ 30 psec) found in the literature.¹⁸ In order to account for some significantly shorter lifetimes obtained in more recent experiments,^{19–21} we have also considered several progressively smaller $\tau_{\text{op}}(0)$ values, as will be discussed in Sec. III. In accordance with the experimental finding of comparable LO and TO Raman linewidths,¹⁹ $\tau_{\text{TO}} = \tau_{\text{LO}}$ was used throughout.

With Eqs. (12) and (16) the phonon Boltzmann equation, Eq. (11), assumes the form of a linear first-order differential equation with coefficients depending on time through the dependence of the emission and absorption rates Eqs. (13) and (14) on T_c , μ_e , and μ_h . The instantaneous phonon distribution for each mode is therefore given by the general solution^{7,22}

$$N_j(t) = \exp \left[- \int_0^t \frac{ds}{\Theta_j(s)} \right] \times \left[\int_0^t ds \frac{\bar{N}_j(s)}{\Theta_j(s)} \exp \left[\int_0^s \frac{d\sigma}{\Theta_j(\sigma)} \right] + N_j^{(0)} \right]. \quad (18)$$

The total scattering rate

$$\frac{1}{\Theta_j(t)} = \frac{1}{\tau_j} + \frac{1}{\tau_{j-c}(t)} \quad (19)$$

is the sum of the lattice-dynamical decay rate τ_j^{-1} in Eq. (16) and the rates for phonon-carrier scattering

$$\frac{1}{\tau_{j-c}(t)} = \sum_s^{e,h} \sum_i^{\text{coupling}} [A_{ij}^{(s)}(t) - E_{ij}^{(s)}(t)]. \quad (20)$$

\bar{N} denotes the asymptotic solution of Eq. (3),

$$\bar{N}_j = \Theta_j \left[\frac{N_j^{(0)}}{\tau_j} + \frac{N_{c,j}}{\tau_{j-c}} \right], \quad (21)$$

for fixed carrier parameters T_c , μ_e , and μ_h ; it shows the tendency of the nonelectronic phonon dynamics to establish the equilibrium Planck distribution $N_j^{(0)}$ with the lattice temperature T_L and of the phonon-carrier interactions to enforce a Planck distribution $N_{c,j}$ heated to the carrier temperature T_c . It is obvious from Eqs. (18) to (21) that in general the phonon distributions are not Planck-type, in which case no phonon temperature can be defined.

The final task is now the parallel integration of the energy balance, Eq. (1), and of the phonon Boltzmann equation, Eq. (11), where the chemical potentials must be determined from the instantaneous carrier densities and carrier temperatures. After each time step, the resulting $E(t)$ determines the new carrier temperature for the next time interval. In this way one obtains the carrier temperature and the phonon distributions as functions of time.

Table I gives definitions and numerical values for material parameters used in our numerical analysis.

III. RESULTS FOR PICOSECOND PULSES

Figure 1 shows experimental carrier temperatures as functions of time after short-pulse laser excitation. The theoretical curves were obtained for the experimental conditions $h\nu = 1.65$ eV, $t_p = 0.5$ psec, and $T_L = 10$ K of Ref. 1, as represented by the solid and open circles. The earlier attempts in Ref. 1 to fit these temperatures with theoretical cooling rates for LO phonon and acoustic phonon scattering led to the result that even after the inclusion of free-carrier screening, additional *ad hoc* reductions of 50% of the phonon-emission rates were necessary to obtain agreement with experiment, and it was suggested that nonequilibrium LO phonon effects might account for these discrepancies.

The solid lines represent the $T_c(t)$ curves obtained from our solution of Eqs. (1) and (11). As was shown in Sec. II,

TABLE I. Material parameters for GaAs (in the standard notation of Refs. 5 and 7).

Definition	Symbol	Value
Mass density	ρ	5.36 g/cm ³
Energy gap	E_g	1.5 eV
Effective masses	m_e	0.067 m_0
	m_h	0.60 m_0
Mean sound vel.	c	3.57×10^5 cm/sec
Acoustic deformation potential	E_0^a	8.6 eV
	E_0^h	3.5 eV
Piezoelectric coupling	F/c^2	4.18×10^{-3}
Optical deformation potential	d_0	41 eV
Overlap correction	K_p^h	2.5
LO phonon energy	$\hbar\omega_{\text{LO}}$	36.2 meV
TO phonon energy	$\hbar\omega_{\text{TO}}$	33.3 meV
Static dielectric constant	ϵ_0	12.91
Optical dielectric constant	ϵ_∞	10.91
Average ϵ_0 for PZ coupling	$\langle \epsilon_0 \rangle_{\text{PZ}}$	12.5

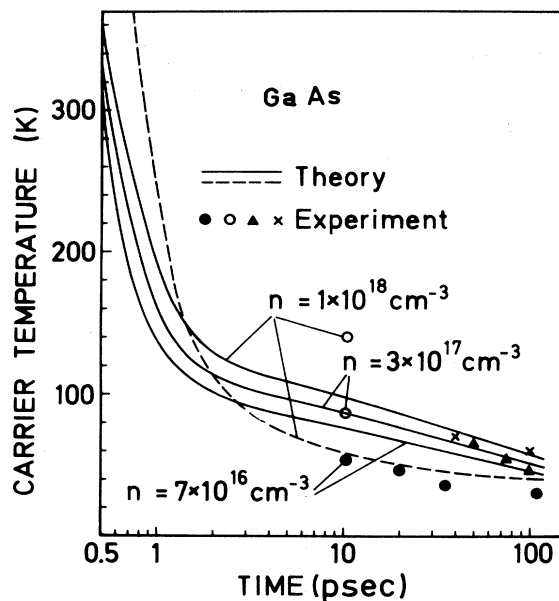


FIG. 1. Carrier temperature as function of time. Experiment: solid circles; Ref. 1, $n = 7 \times 10^{16} \text{ cm}^{-3}$; open circles, Ref. 1, $n = 3 \times 10^{17} \text{ cm}^{-3}$ and $1 \times 10^{18} \text{ cm}^{-3}$; triangles, Ref. 2; crosses, Ref. 3. Theory: solid lines for optical phonon disturbances, dashed line for equilibrium phonons.

these calculations were free of any adjustable parameter and included not only the energy loss of electrons and holes to LO modes through the polar-optical interaction, but also of the holes to TO modes through the intrinsically much weaker optical-deformation potential coupling.

There is very good agreement between the theoretical curve for $n = 3 \times 10^{17} \text{ cm}^{-3}$ and the experimental point at 10 psec. For the two other cases of $n = 7 \times 10^{16} \text{ cm}^{-3}$ and $1 \times 10^{18} \text{ cm}^{-3}$, the fit of the transmission data had been less accurate (see Fig. 2 of Ref. 1), so that the remaining discrepancies of roughly +40% and -30% between our theory and the experimental data may be partly caused by deviations of the photoexcited carrier distributions from the Fermi-Dirac form and corresponding uncertainties in the experimentally determined carrier temperatures. As far as the calculations are concerned, the detailed form of the carrier distribution functions has little influence on the overall energy relaxation of the carriers, Eq. (1).²²

We note from Fig. 1 that the heating of optical phonons indeed seems to explain the slow carrier cooling, because even after inclusion of TO scattering as a further energy relaxation mechanism our theoretical carrier temperatures are higher than in the previous calculations¹ for phonon equilibrium and for LO-phonon emission only. However, in order to provide a better insight into the phonon dynamics, Fig. 2 shows the carrier temperature and the phonon distribution function of a strongly coupling LO mode and TO mode during and after the laser pulse for the case of $n = 1 \times 10^{18} \text{ cm}^{-3}$.

$N_{LO}(t)$ shows a behavior quite expected from the picture of the initial emission of optical phonons followed by their subsequent decay into pairs of lower-lying phonons

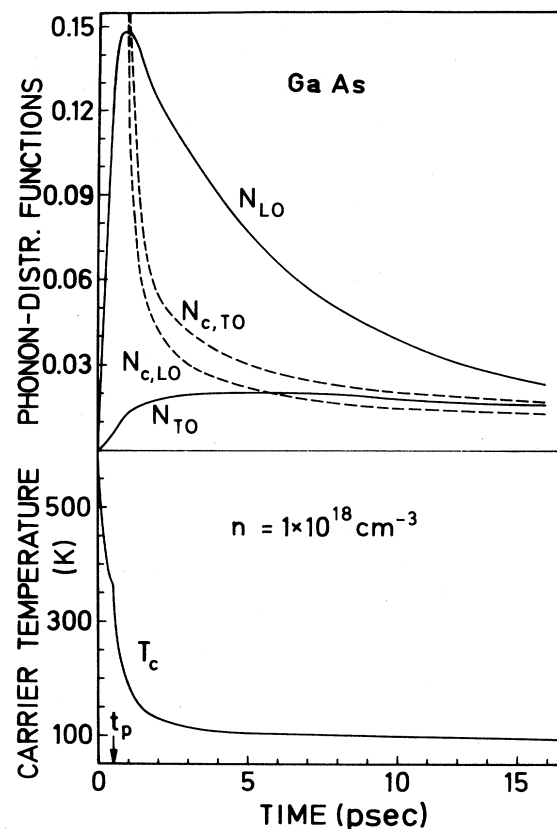


FIG. 2. Theoretical phonon distributions and heated Planck distributions as functions of time for $n = 1 \times 10^{18} \text{ cm}^{-3}$, $q_{LO} = 3.4 \times 10^6 \text{ cm}^{-1}$, and $q_{TO} = 5.5 \times 10^6 \text{ cm}^{-1}$.

after the end of the pulse. But the comparison of their lattice-dynamical lifetime of 26 psec used in the calculation with the apparent decay time of about 5 psec in Fig. 2 makes it obvious that carrier-phonon processes must have dominated this LO-phonon relaxation. Indeed a closer inspection of the partial cooling rates for polar-optical and optical-deformation potential processes as functions of time reveals the following sequence of events.

In contrast to the more weakly coupling TO modes, the LO phonons of small wave vector are already strongly amplified during the pulse so that carrier cooling through the PO coupling becomes more and more reduced. Since the lattice-dynamical decay rate of the LO phonons is smaller than the cooling rate, which is already dominated by TO-phonon emissions, and therefore smaller than the corresponding decrease of the heated Planck distribution $N_{c,LO}$, roughly half a psec after the pulse the value of $N_{c,LO}$ has fallen below the actual distribution N_{LO} of the initially amplified LO phonons. Since quite generally the "detailed-balance" value N_c denotes the borderline between predominant emission ($N < N_c$) or absorption ($N > N_c$) of the phonons by the carriers, energy and momentum will now be fed back from the LO modes to the carrier system through reabsorption processes. It is exactly this reabsorption dynamics and not the lattice-

dynamical LO-phonon lifetime that causes the rapid decay of the LO-phonon population.

On the other hand the disturbance of TO phonons, also represented in Fig. 2 by one of their most strongly coupling modes, is much weaker, so that $N_{c,TO}(t)$ is always larger than the instantaneous TO distribution. During the LO-phonon reabsorption phase the carrier cooling is therefore driven by the emission of TO phonons by holes through the practically unscreened optical deformation-potential coupling.

So screening plays a minor role in the energy transfer to the lattice. In fact, it even accelerates the carrier cooling for the following reason: The slowing down of the cooling is caused by the reabsorption of the initially amplified LO phonons. Any phonon disturbance is directly proportional to the number of carriers, if screening effects are neglected. But the actual screening of the polar couplings will weaken this proportionality, thereby decrease the number of initially excited phonons and consequently diminish the retarding action of the reabsorption mechanism.

A more detailed analysis of the role of certain physical parameters and model assumptions is summarized in Table II. Modification 1 represents the standard case, $n(t_p) = 1 \times 10^{18} \text{ cm}^{-3}$, with the most relevant input data listed in the heading of the table. The modifications 2–8 show the results obtained for different choices of certain input parameters, whose values are listed in the second column.

Line 1 for the standard case contains the carrier temperature as function of time, as also shown in Figs. 1 and 2. Since the time integration of the coupled carrier-phonon system starts from $t=0$, all effects of phonon disturbances, including those during the laser pulse, are taken into account. Line 4 contains the analogous results for phonon equilibrium, also shown in Fig. 1. Line 5, again for phonon equilibrium, was obtained for a gap value of 1.53 eV, with a resulting excess energy $h\nu - E_g$ per electron-hole pair of 120 meV, as compared to 150 meV for the standard case. Modifications 4 and 5 follow the usual approaches¹ of starting the time integration at the end of the pulse, estimating the energy content $E(t_p)$ and the corresponding carrier temperature $T_c(t_p)$ from the pair-generation rate and the excess energy per excited pair

by neglecting lattice losses during the pulse. A comparison of lines 4 and 5 shows the small dependence of the carrier cooling on the detailed gap value and the resulting initial carrier temperature. This small influence is also found when phonon disturbances are taken into account. For this reason effects of band-gap renormalization were not included in our analysis.

Modifications 1–3 for progressively smaller values of the phonon lifetime τ_{op} should be compared with case 4 for phonon equilibrium, which corresponds to $\tau_{op}=0$. From Eq. (20) the electronic emission and absorption rates are found to be typically of the order of several ten psec^{-1} ; only if the decay rates τ_{op}^{-1} of the excited phonons were markedly larger could the effects of phonon disturbances by the carriers be neglected. This would require unrealistically small optical-phonon lifetimes of at most a few picoseconds. Indeed, even the very small value of $\tau_{op}=4 \text{ psec}$ (case 3) leads to carrier temperatures which for the first 10 psec are still half-way between those for $\tau_{op}=26 \text{ psec}$ and those for phonon equilibrium (case 4).

Line 6 was obtained for an optical deformation potential $d_0=29 \text{ eV}$,^{2,3} which amounts to a 50% reduction of the standard value for the ODP transition amplitudes in Eq. (15). The important role of the TO phonons is reflected by the fact that the smaller ODP results in a markedly higher carrier temperature during and immediately after the laser pulse. Line 7 shows that Thomas-Fermi screening of the optical deformation potentials, although physically unjustified, would have very little effect because of the short range of the interaction.

The irrelevance of the details of the free-carrier screening in the presence of strong phonon disturbances is most clearly demonstrated by modification 8, in which all couplings, including the long-range polar optic interaction, were left completely unscreened. Already 1 psec after the end of the excitation pulse, the carrier temperatures are practically the same as in case 1 for the actual screening conditions. This at first sight surprising effect has already been mentioned in our discussion of Fig. 2: As compared to case 1, the unscreened PO couplings lead to a stronger initial LO-phonon amplification, resulting in the lower carrier temperature at the end of the pulse; however, the correspondingly stronger reabsorption of these phonons leads to a lower cooling rate after the pulse, so that the re-

TABLE II. Dependence of carrier cooling on computational procedure and choice of parameters. Standard case: GaAs, $T_L=10 \text{ K}$, $h\nu=1.65 \text{ eV}$, $\tau_p=0.5 \text{ psec}$, $n(t_p)=1 \times 10^{18} \text{ cm}^{-3}$; PO coupling TF screened; ODP, $d_0=41 \text{ eV}$, unscreened; $\tau_{op}(T_L=0)=26 \text{ psec}$; $\tau_{rec}=1 \times 10^{-9} \text{ sec}$.

Modification	Integrated from	Carrier temperature $T_c(t)$					
		$t \text{ (psec)}=0.5$	1.5	5.5	10.5	35.5	110.5
1 Standard	$t=0$	366	147	108	98	77	56
2 $\tau_{op}(0)=13 \text{ psec}$	$t=0$	365	147	105	92	66	49
3 $\tau_{op}(0)=4 \text{ psec}$	$t=0$	365	145	93	76	53	44
4 Phonon equil.	$t=t_p$	580	147	71	60	47	41
5 Phonon equil. $E_g=1.53 \text{ eV}$	$t=t_p$	465	137	70	59	47	41
6 $d_0=29 \text{ eV}$	$t=0$	404	178	120	107	81	58
7 ODP screened	$t=0$	372	158	114	103	79	58
8 no PO screening	$t=0$	341	152	111	99	77	54

sulting carrier temperatures for $t > 1.5$ psec are even higher than for the screened PO couplings. It is this counterbalance of any screening-induced change of the carrier-phonon couplings by the corresponding change in the phonon disturbances which leaves the nonequilibrium phonon effects as the determining factor for the strong retardation of the energy transfer to the lattice.

IV. RESULTS FOR NANOSECOND PULSES

The central result of the preceding Sec. III, namely that the slowing down of the carrier cooling is mainly determined by nonequilibrium phonon effects, is typical for the moderate carrier densities generated by the ultrashort excitation pulses of Refs. 1–4. A further increase of the pair density n will eventually lead to an outweighing of the proportionality of the phonon amplification to n by the approximate n^2 dependence of the square of the dielectric function in the denominator of the transition amplitudes $B_{\text{PO, (LO)}}^{(s)}$ in Eq. (15).⁵ For the very high plasma densities found in pulsed-laser annealing, the relative importance of LO-phonon disturbances might therefore be strongly reduced.²⁴

To get a first information about the carrier-phonon dynamics for higher carrier densities we have simulated a quasi-cw excitation by choosing an excess energy per excited e - h pair of ≈ 818 meV, corresponding to a temperature $T_c(0) = 3158$ K for initially excited (still nondegenerate) carriers.⁴ The laser pump rate, G_0 in Eq. (4), was assumed to be $10^{31} \text{ cm}^{-3} \text{ sec}^{-1}$. Table III shows the pair density, carrier temperature, the change of the pair generation rate G due to band filling, and the distribution functions of a representative LO and TO mode as func-

tions of time. The time integration of Eqs. (1) and (11) was terminated, when a quasi-steady-state was reached.²⁵ The final plasma densities of $5 \times 10^{19} \text{ cm}^{-3}$ were still 1 order of magnitude below the typical values of $10^{20} - 10^{21} \text{ cm}^{-3}$ for laser annealing.

The very rapid decrease of the carrier temperature during the first 10 psec is a direct consequence of the particle statistics: Even if we neglected phonon emissions, the condition of constant energy per particle would give such a strong weight to the high-energy portion of the distribution functions that the increase of the chemical potentials during the creation of new carriers would necessarily lead to a narrowing of the thermal width of the distributions, resulting in a decrease of T_c . This leaves the initially amplified phonons “superthermal” with respect to the carriers for times between 5 and 10 psec after the onset of the pulse, as can be seen from $N > N_c$ for both modes.

The final steady state of the carrier system is determined by the balance between the pair excitation, the free-carrier absorption, and Auger processes with the recombination losses and the lattice losses. The latter are strongly reduced by the phonon disturbances, because the asymptotic solutions of Eq. (11) are very near to the heated Planck distributions, as shown in Table III for the two representative modes of our example. The by-far dominant lattice losses of the carrier system are TO-phonon emissions, with a few percent contributions from losses to LO phonons (through the strongly screened polar coupling) and to acoustic phonons.

The contributions of Auger recombination and free-carrier absorption to the final carrier temperature turned out to be only a few percent, justifying their approximate treatment in our analysis. However, under laser-annealing

TABLE III. Approach to a steady state during quasicontinuous laser excitation of GaAs (theory): standard material parameters; $\tau_{\text{rec}} = 10^{-10} \text{ sec}$; laser pump rate, $G_0 = 1.10^{31} \text{ cm}^{-3} \text{ sec}^{-1}$; $T_c(0) = 3158 \text{ K}$.

t (psec)	n (10^{19} cm^{-3})	T_c (K)	G ($10^{31} \text{ cm}^{-3} \text{ sec}^{-1}$)	$T_L = 10 \text{ K}$		$T_L = 300 \text{ K}$	
				N_{LO} $q_{\text{LO}} = 0.8 \times 10^7 \text{ cm}^{-1}$	$N_{c,\text{LO}}$ $q_{\text{LO}} = 0.8 \times 10^7 \text{ cm}^{-1}$	N_{TO} $q_{\text{TO}} = 1.3 \times 10^7 \text{ cm}^{-1}$	$N_{c,\text{TO}}$ $q_{\text{TO}} = 1.3 \times 10^7 \text{ cm}^{-1}$
2.5	2.39	698	0.850	1.085	1.223	0.264	1.354
5.	4.18	369	0.636	0.644	0.477	0.458	0.542
7.5	5.00	299	0.144	0.374	0.330	0.412	0.379
10.	5.07	282	0.055	0.297	0.295	0.353	0.341
22.5	5.06	250	0.051	0.223	0.232	0.257	0.271
35.	5.06	239	0.051	0.200	0.212	0.231	0.248
47.5	5.06	232	0.051	0.189	0.198	0.217	0.234
60.	5.06	229	0.051	0.183	0.193	0.210	0.227
72.5	5.06	227	0.051	0.179	0.189	0.206	0.223
2.5	2.39	833	0.853	1.277	1.539	0.596	1.697
5.	4.17	477	0.614	0.849	0.716	0.706	0.802
7.5	4.98	404	0.178	0.579	0.553	0.631	0.625
10.	5.10	381	0.065	0.497	0.503	0.564	0.570
22.5	5.10	347	0.051	0.416	0.430	0.468	0.490
35.	5.09	341	0.052	0.402	0.417	0.453	0.476
47.5	5.09	339	0.052	0.399	0.413	0.450	0.471
60.	5.09	339	0.052	0.399	0.413	0.449	0.471
72.5	5.09	339	0.052	0.399	0.413	0.449	0.471

conditions the power input from these higher-order processes, and also from two-photon absorption, would be comparable to or larger than the energy gain of the carrier system from direct one-photon interband absorption.

The present theory could be extended to describe the electronic power transfer under the conditions of pulsed-laser annealing, because the transport formulation allows for the inclusion of collective plasma effects and carrier diffusion. The stepwise decay of the initially excited phonons into the heat bath of the thermal phonon reservoir could in principle also be incorporated by adding the coupled rate equations for the phonons along the relaxation path. Since this energy transfer to the lattice is the fundamental process of all thermal-annealing models, and in view of the still controversial alternative of a nonthermal-annealing mechanism,²⁶ theoretical and experimental analysis of the phonon cascade would be highly desirable.

V. CONCLUSION

A detailed time-resolved transport analysis of photogenerated carrier-phonon systems in GaAs has been given, leading to new insights into the role of phonon disturbances in laser-excited polar semiconductors. These findings justify the complexity of the present approach by correcting our physical picture of the mutual role of free-carrier screening and optical-phonon amplification. In addition to the physical requirement of a consistent treatment of the coupled nonequilibrium carrier and phonon systems, there has been ample evidence for strong amplification of laser-excited optical phonons in the picosecond Raman spectroscopy of various polar semiconductors.¹⁶ The theory is free of adjustable parameters in the sense that only experimentally determined and generally accepted material parameters were used in the numerical calculations.²⁷

For picosecond or subpicosecond laser pulses of moderate power densities ($\leq 3 \times 10^8 \text{ W cm}^{-2}$) and electron-hole pair concentrations between $5 \times 10^{16} \text{ cm}^{-3}$ and $1 \times 10^{18} \text{ cm}^{-3}$ the following is shown.

(i) Amplification of LO phonons and the resulting quenching of LO-phonon emissions by the carriers is the decisive mechanism for the slowing down of the energy

transfer from the initially excited hot carriers to the lattice. The plasma cooling after the end of the laser pulse is in fact only caused by the emission of TO phonons by holes, in contrast to the earlier expectations that the intrinsically weaker coupling to TO phonons can be neglected.¹

(ii) The reduction of the polar carrier-phonon couplings to the increased free-carrier screening does *not* retard the carrier cooling, because it is counterbalanced by the correspondingly smaller LO-phonon amplification. This is again in contrast to the original interpretations of the experimental data,¹ in which screening effects were estimated under the assumption of phonon equilibrium, and LO-phonon heating was supposed to be an independent additional retardation mechanism; in this way free-carrier screening was erroneously obtained as the major cause for the reduction of the carrier cooling.

(iii) The rate for the reabsorption of the initially excited LO phonons by the photo-induced carriers after the end of picosecond or subpicosecond laser pulses is several times faster than the lattice-dynamical decay rate of these phonons. This has consequences for any time-resolved laser spectroscopy of LO phonons under experimental conditions similar to those of Ref. 1: The apparent decay times, if interpreted as intrinsic phonon lifetime, will give only a fraction of the actual value. This might explain the large discrepancy between experimentally determined LO-phonon lifetimes found in the literature.

A similar reduction of the carrier-cooling due to LO- and also of TO-phonon disturbances must be expected for quasi-cw excitation and plasma densities of up to several 10^{19} cm^{-3} .

For the very high excitation densities under laser-annealing conditions the much larger free-carrier screening will strongly suppress any LO-phonon amplification, justifying the assumption of an equilibrium phonon distribution in earlier screening theories.¹⁵

ACKNOWLEDGMENTS

This work was supported by the Fonds zur Förderung der wissenschaftlichen Forschung in Österreich, Projekt Nr. SS-22/07.

*Present address: Department of Electrical Engineering, Colorado State University, Fort Collins, CO 80523.

¹R. F. Leheny, J. Shah, R. F. Fork, C. V. Shank, and A. Migus, *Solid State Commun.* **31**, 809 (1979); see also J. Shah, *J. Phys. (Paris)* **42**, C7-445 (1981).

²D. von der Linde and R. Lambrich, *Phys. Rev. Lett.* **42**, 1090 (1978).

³S. Tanaka, H. Kobayashi, H. Saito, and H. Shionoya, *J. Phys. Soc. Jpn.* **49**, 1051 (1980).

⁴E. O. Göbel and O. Hildebrand, *Phys. Status Solidi B* **88**, 645 (1978); W. Graudszus and E. O. Göbel, in *Proceedings of the 16th International Conference on Semiconductors, Montpel-*

lier, 1982, edited by M. Averous (North-Holland, Amsterdam, 1983), p. 555.

⁵M. Pagnet, J. Collet, and A. Cornet, *Solid State Commun.* **38**, 531 (1981).

⁶H. M. van Driel, *Phys. Rev. B* **19**, 5928 (1979).

⁷P. Kocevar, *J. Phys. C* **5**, 3349 (1972).

⁸J. H. Bechtel and W. L. Smith, *Phys. Rev. B* **13**, 3515 (1976).

⁹E. J. Johnson, in *Semiconductors and Semimetals*, edited by R. K. Willardson and A. C. Beer (Academic, New York, 1975), Vol. III, p. 153.

¹⁰A. Elci, M. Scully, A. L. Smirl, and J. C. Matter, *Phys. Rev. B* **16**, 191 (1977).

- ¹¹G. Benz and R. Conrat, *Phys. Rev. B* **16**, 843 (1977).
- ¹²R. Stratton, *Proc. R. Soc. London Ser. A* **246**, 406 (1958).
- ¹³J. Collet, A. Cornet, M. Pugnet, and T. Amand, *Solid State Commun.* **42**, 883 (1982).
- ¹⁴Sh. M. Kogan, *Fiz. Tverd. Tela Leningrad* **4**, 2474 (1962) [*Sov. Phys.—Solid State* **4**, 1813 (1963)].
- ¹⁵E. J. Yoffa, *Phys. Rev. B* **21**, 2415 (1980); **23**, 1909 (1981).
- ¹⁶For a review of experimental phonon lifetimes, see P. Kocevar, in *Physics of Nonlinear Transport in Semiconductors*, edited by D. K. Ferry, J. R. Barker, and C. Jacoboni (Plenum, New York 1980), p. 401.
- ¹⁷P. G. Klemens, *Phys. Rev.* **148**, 845 (1966).
- ¹⁸A. Mooradian and G. B. Wright, *Solid State Commun.* **4**, 431 (1966).
- ¹⁹R. K. Chang, J. M. Ralston, and D. E. Keating, *Proceedings of the International Conference Scattering Spectra in Solids*, edited by G. B. Wright (Springer, New York, 1969), p. 369.
- ²⁰D. von der Linde, J. Kuhl, and H. Klingenberg, *Phys. Rev. Lett.* **44**, 1505 (1980).
- ²¹J. Shah, R. C. C. Leite, and J. F. Scott, *Solid State Commun.* **8**, 1089 (1970).
- ²²P. Kocevar, W. Pötz, and W. Porod, in *Proceedings of the 16th International Conference on Semiconductors, Montpellier, 1982*, edited by M. Averous (North-Holland, Amsterdam, 1983), p. 220.
- ²³W. Pötz and P. Vogl, *Phys. Rev. B* **24**, 2025 (1981).
- ²⁴Much smaller effects of LO phonon disturbances can also be expected for very high picosecond excitation densities, as, e.g., for the recent time-resolved luminescence data of R. J. Seymour, M. R. Junnarkar, and R. R. Alfano, *Solid State Commun.* **41**, 657 (1982).
- ²⁵The number of time steps for sufficient accuracy of the time integration was of the order of 1000 for the first 100 psec.
- ²⁶J. A. Van Vechten and R. Tsu, *Phys. Lett.* **74A**, 422 (1979); H. W. Lo and A. Compaan, *Phys. Rev. Lett.* **44**, 1604 (1980).
- ²⁷Our arbitrary choice of setting the coefficient for free-carrier absorption for GaAs equal to that of germanium has negligible consequences for picosecond excitation and does not influence our conclusions for cases of quasi-cw excitation.